

Article

Two Congeneric Shrubs from the Atacama Desert Show Different Physiological Strategies That Improve Water Use Efficiency under a Simulated Heat Wave

Enrique Ostría-Gallardo ^{1,*} , Estrella Zúñiga-Contreras ^{1,2}, Danny E. Carvajal ^{3,4,5}, Teodoro Coba de La Peña ² , Ernesto Gianoli ⁶ and Luisa Bascuñán-Godoy ⁷ 

- ¹ Laboratory of Plant Physiology, Center of Advanced Studies in Arid Zones (CEAZA), La Serena 1700000, Chile; estrelladelpilar@gmail.com
- ² Laboratory of Phytoremediation, Center of Advanced Studies in Arid Zones (CEAZA), La Serena 1700000, Chile; teodoro.cobadelapena@ceaza.cl
- ³ Laboratory of Plant Ecophysiology, Department of Biology, Universidad de La Serena, La Serena 1700000, Chile; dcarvajal@userena.cl
- ⁴ Instituto de Ecología y Biodiversidad (IEB), Santiago 8320000, Chile
- ⁵ Centro de Ciencia del Clima y la Resiliencia, CR2, Santiago 8320000, Chile
- ⁶ Laboratory of Functional Ecology, Department of Biology, Universidad de La Serena, La Serena 1700000, Chile; egianoli@userena.cl
- ⁷ Laboratory of Plant Physiology, Department of Botany, Universidad de Concepción, Concepción 4030000, Chile; lubascun@udec.cl
- * Correspondence: enrique.ostría@ceaza.cl; Tel.: +56-51-2204378



Citation: Ostría-Gallardo, E.; Zúñiga-Contreras, E.; Carvajal, D.E.; de La Peña, T.C.; Gianoli, E.; Bascuñán-Godoy, L. Two Congeneric Shrubs from the Atacama Desert Show Different Physiological Strategies That Improve Water Use Efficiency under a Simulated Heat Wave. *Plants* **2023**, *12*, 2464. <http://doi.org/10.3390/plants12132464>

Academic Editors: Chien Van Ha, Swarup Roy Choudhury, Mohammad Golam Mostofa and Gopal Saha

Received: 23 May 2023

Revised: 16 June 2023

Accepted: 21 June 2023

Published: 28 June 2023



Copyright: © 2023 by the authors. Licensee MDPI, Basel, Switzerland. This article is an open access article distributed under the terms and conditions of the Creative Commons Attribution (CC BY) license (<https://creativecommons.org/licenses/by/4.0/>).

Abstract: Desert shrubs are keystone species for plant diversity and ecosystem function. *Atriplex clivicola* and *Atriplex deserticola* (Amaranthaceae) are native shrubs from the Atacama Desert that show contrasting altitudinal distribution (*A. clivicola*: 0–700 m.a.s.l.; *A. deserticola*: 1500–3000 m.a.s.l.). Both species possess a C4 photosynthetic pathway and Kranz anatomy, traits adaptive to high temperatures. Historical records and projections for the near future show trends in increasing air temperature and frequency of heat wave events in these species' habitats. Besides sharing a C4 pathway, it is not clear how their leaf-level physiological traits associated with photosynthesis and water relations respond to heat stress. We studied their physiological traits (gas exchange, chlorophyll fluorescence, water status) before and after a simulated heat wave (HW). Both species enhanced their intrinsic water use efficiency after HW but via different mechanisms. *A. clivicola*, which has a higher LMA than *A. deserticola*, enhances water saving by closing stomata and maintaining RWC (%) and leaf Ψ_{md} potential at similar values to those measured before HW. After HW, *A. deserticola* showed an increase of A_{max} without concurrent changes in g_s and a significant reduction of RWC and Ψ_{md} . *A. deserticola* showed higher values of Chl *a* fluorescence after HW. Thus, under heat stress, *A. clivicola* maximizes water saving, whilst *A. deserticola* enhances its photosynthetic performance. These contrasting (eco)physiological strategies are consistent with the adaptation of each species to their local environmental conditions at different altitudes.

Keywords: *Atriplex*; Atacama Desert; C4 pathway; desert shrubs; heat wave; gas exchange; chlorophyll fluorescence

1. Introduction

Desert shrubs constitute a distinct physiognomic and ecological group with characteristic morphological and physiological adaptations [1,2]. Further, they often play a key role in the maintenance of plant diversity by acting as nurse plants [3] and may even impact ecosystem processes [4]. In the context of climate change and its profound effects on the physiology, phenology, abundance and distribution of species [5–10], it is essential to understand the mechanisms by which desert shrubs deal with climate change components.

Climate change involves not only increased temperature averages but also increased occurrence of climatic anomalies, such as heat waves [11]. In fact, heat waves are becoming increasingly frequent, more intense and broader in spatial extent [12–14]. Temperature controls the distribution, productivity, and physiological activity of plants, both at spatial and temporal scales [15,16]. Although they consist of relatively short events, heat waves may have significant ecological impacts and cause long-term ecological shifts [17,18]. Heat waves have been shown to affect plant physiological processes, such as the efficiency of photosystem II, stomatal conductance and leaf water potential [13,19,20]. Despite an increasing number of studies, the understanding of the effects of heat waves on plants is still fragmentary [13].

In eudicots, those with a C4 photosynthetic pathway are considered more tolerant to heat and water stress than C3 species because they have higher water-use efficiencies and negligible effects of heat on photorespiration [21,22]. Among predominantly C4 clades, the *Atriplex* genus (Amaranthaceae) is the largest one, including over 300 C4 species [23]. The *Atriplex* genus has spread worldwide, being mainly distributed across arid subtropical and temperate regions, particularly in harsh inland and coastal habitats [24]. Consequently, *Atriplex* species are usually labeled as highly tolerant plants against abiotic stresses, especially drought and salinity [25,26]. Adaptations to desert conditions in *Atriplex* shrubs leading to improved water economy have long been studied, including low mesophyll resistance and high stomatal resistance in *A. spongiosa* [27], steeply angled leaves during midday in *A. hymenelytra* [28], increased Na⁺ uptake in *A. halimus* [29], and increased osmotic adjustment in *A. nummularia* [30]. Furthermore, header books of plant (eco)physiology include *Atriplex* species when describing tolerance to high temperatures [31,32]. Nevertheless, little is known about their response to heat stress [33], much less about their response to heat waves.

Forty-six *Atriplex* species have been reported in Chile, most of them distributed in arid and semi-arid regions, which have experienced changes in the trends of heat waves and maximum temperatures [34,35]. During the 1961–2016 period, it was observed an increase in the number and duration of heat wave events [34]. Additionally, during the 1979–2015 period, there was an increase in maximum temperatures for summer and autumn, and high-altitude areas experienced a greater increase in maximum temperatures compared to lower and coastal areas [35]. Among the native *Atriplex* species inhabiting (semi)arid Chile, *Atriplex clivicola* and *A. deserticola* are two phylogenetically-close perennial endemic shrubs from the Atacama Desert [36,37]. These species share most of their latitudinal distribution but differ greatly in their altitudinal distribution [37]. *Atriplex clivicola* mainly inhabits coastal to lowland areas, from sea level up to 700 m a.s.l, whereas *A. deserticola* inhabits highlands from 1500 up to 3000 m a.s.l. Both species have a C4 photosynthetic pathway and Kranz anatomy, traits adaptive to high temperatures. However, besides sharing a C4 pathway, it is not clear how their leaf-level physiological traits associated with photosynthesis and water relations respond to heat stress. Here, we addressed whether *A. clivicola* and *A. deserticola* would enhance or maintain their leaf water status while maintaining carbon assimilation under a heat wave event. We evaluated gas exchange, chlorophyll *a* fluorescence, and leaf water status before and after a simulated heat wave. The overarching goal of this study was to study the strategies leading to water use efficiency in two representative desert shrubs under conditions of a heat wave, which is one of the components of current climate change.

2. Results

2.1. Chlorophyll *a* Fluorescence

The *Atriplex* species did not differ in the Fv/Fm parameter before or after HW. However, within species, Fv/Fm showed a significant reduction after HW yet maintained values above 0.7 (Figure 1A). The actual quantum yield (Φ PSII) only showed differences between species after HW, being lower in *A. clivicola* (Figure 1B). On the other hand, the quantum yield of energy dissipation (Fo/Fm) was higher in *A. deserticola* than in *A. clivicola* only

before HW. The former reduced F_o/F_m significantly after HW, whereas similar values to those before HW were observed in *A. clivicola* (Figure 1C).

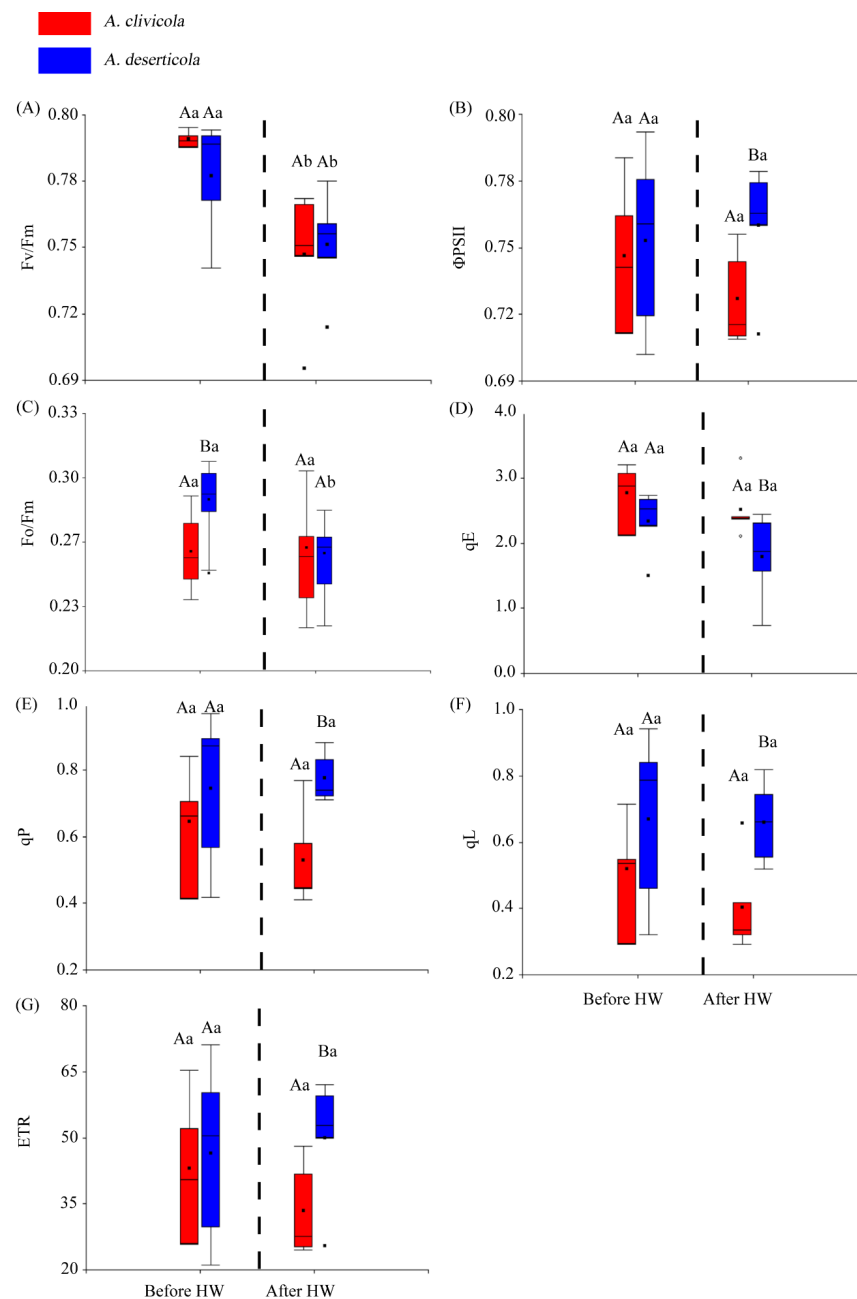


Figure 1. Box plots for the chlorophyll *a* fluorescence parameters of *Atriplex clivicola* (red; $n = 12$ individuals) and *Atriplex deserticola* (blue; $n = 12$ individuals) species before and after the simulated heat wave (HW). The dashed line of each plot separates the values obtained before and after HW. The black dot and horizontal line inside each box indicates the mean and median values. Vertical lines outside the box indicate the extreme lower and upper values of the dataset. Upper case letters indicate significant differences between species before and after HW. Lowercase letters indicate significant differences within species when values before and after HW are compared. F_v/F_m Maximum quantum efficiency of photosystem II (A); Φ_{PSII} Actual quantum yield of photosystem II (B); F_o/F_m Quantum yield of energy dissipation at time = 0 (C); qE Quenching component associated to energy dissipation (D); qP Quenching component associated to photochemistry (E); qL Fraction of open PSII centers (with QA oxidized) on the basis of a lake model for the PSII photosynthetic apparatus (F); ETR Electron transport rate (G).

The components of NPQ, qE, qP and qL (at $p < 0.05$) (Figure 1D–F) showed differences between species after HW. After the HW simulation, the qE values were higher in *A. clivicola*, whilst qP and qL values were higher in *A. deserticola*.

No significant changes in ETR were observed within species before or after HW (Figure 1G). We did find differences in ETR between species, but only after HW, being lower for *A. clivicola*.

2.2. Gas Exchange Variables

The photosynthetic rate (A_{\max}) values showed differences between species only before HW (Figure 2A), being ~47% higher in *A. clivicola* ($14.32 \mu\text{mol CO}_2 \text{ m}^{-2} \text{ s}^{-1}$) than in *A. deserticola* ($9.77 \mu\text{mol CO}_2 \text{ m}^{-2} \text{ s}^{-1}$). After HW, the photosynthetic rate of *A. clivicola* remained similar to values observed before HW. However, the photosynthetic rate of *A. deserticola* increased by 39% after HW.

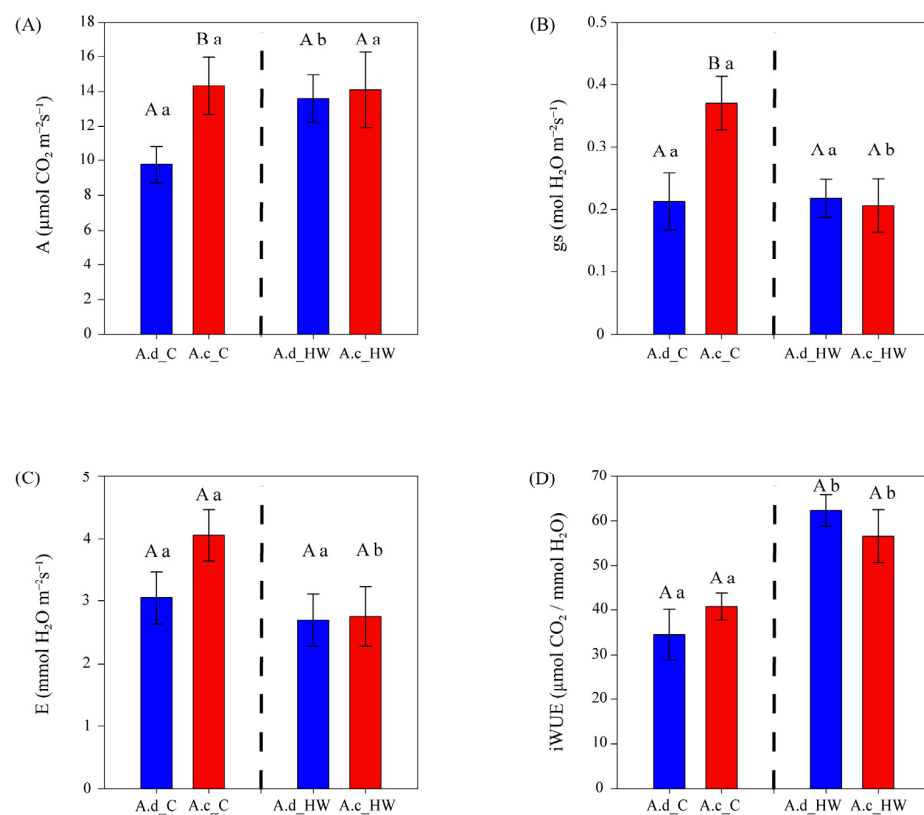


Figure 2. Gas exchange parameters of *A. clivicola* (red; $n = 12$ individuals) and *A. deserticola* (blue; $n = 12$ individuals) before and after the simulated heat wave (HW). The dashed line inside each plot separates the values obtained before and after HW. Bars and vertical lines above the bars indicate the mean and the standard error values, respectively. Upper case letters indicate significant differences between species either before HW or after HW. Lowercase letters indicate significant differences within species when values before and after HW are compared. A Photosynthetic rate at light saturation (A); g_s Stomatal conductance (B); E Transpiration rate (C); iWUE Intrinsic water use efficiency (D).

Stomatal conductance (g_s) was higher in *A. clivicola* than in *A. deserticola* before HW, whilst no difference between species was observed after HW (Figure 2B). *A. deserticola* showed similar values of g_s before and after HW (0.21 and $0.22 \text{ mol H}_2\text{O m}^{-2} \text{ s}^{-1}$, respectively). On the other hand, a significant decrease in g_s (~43%) was observed in *A. clivicola* after HW, reaching similar values to those of *A. deserticola*.

Leaf transpiration $ra(E)$ showed no differences between species either before or after HW (Figure 2C). Within species, *A. clivicola* showed a ~32% decrease in E after HW ($p = 0.0506$), whereas the E of *A. deserticola* was not affected by HW.

The intrinsic water use efficiency (iWUE) was remarkably similar in *A. clivicola* and *A. deserticola* both before and after HW (Figure 3D). Within species, after HW, a significant increase of ca. 39 and 81% in iWUE was observed in *A. clivicola* and *A. deserticola*, respectively (Figure 2D).

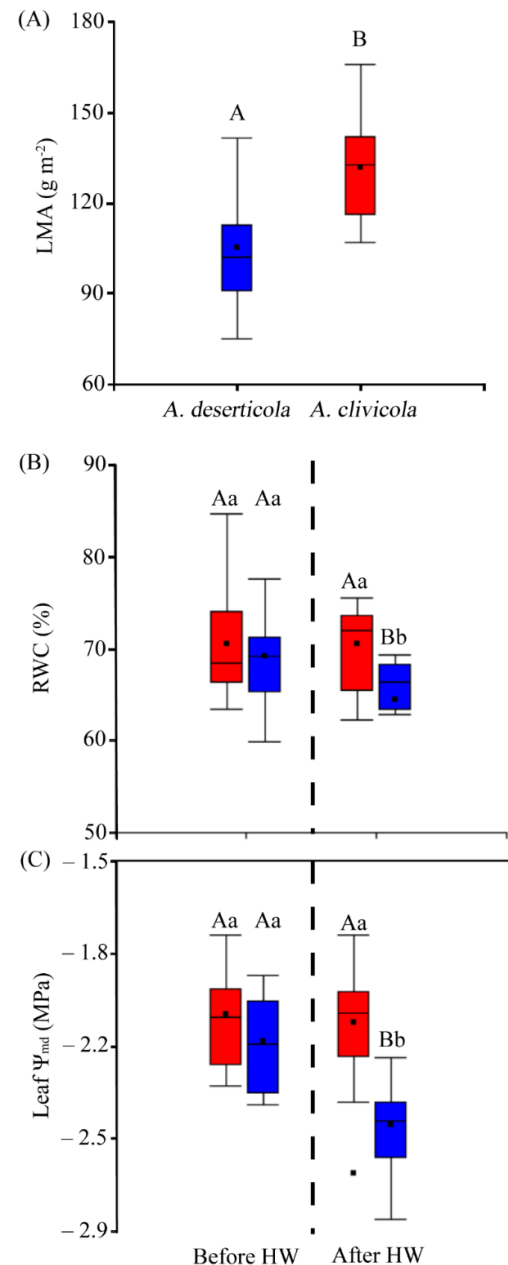


Figure 3. (A) Leaf mass per area (LMA) values of *A. deserticola* ($n = 12$ individuals) and *A. clivicola* ($n = 12$ individuals). (B) The percentage of relative water content (RWC) of *A. clivicola* and *A. deserticola* before and after simulated heat wave (HW). (C) Leaf water potential at midday (Ψ_{md}) of *A. clivicola* and *A. deserticola* before and after the simulated HW. The dashed line inside each plot separates the values obtained before and after HW. The black dot and horizontal line inside the box plots indicates the mean and median values. Vertical lines outside the boxes indicate the extreme lower and upper values of the dataset. Upper case letters indicate significant differences between species either before HW or after HW. Lowercase letters indicate significant differences within species when values before and after HW are compared.

2.3. Photosynthetic Temperature–Response Curves

The optimum photosynthetic temperature (T_{opt}) values differed between species ($p < 0.05$) (Table 1). *A. deserticola* averaged an optimum temperature of 29.63 °C, while *A. clivicola* had an optimum temperature of 27.07 °C. Similarly, the photosynthetic rate at thermal optimum (A_{opt}) was higher ($p < 0.05$) in *A. deserticola* (19.64 $\mu\text{mol CO}_2 \text{ m}^{-2} \text{ s}^{-1}$) than in *A. clivicola* (9.30 $\mu\text{mol CO}_2 \text{ m}^{-2} \text{ s}^{-1}$).

Table 1. Parameters from the photosynthetic temperature–response curves of *A. clivicola* ($n = 4$ individuals) and *A. deserticola* ($n = 4$ individuals). The table depicts the thermal sensitivity of photosynthesis to high temperatures. The values correspond to the average and standard error for the maximum temperature at the carbon compensation point (T_{max}), the optimum temperature for photosynthesis (T_{opt}), the photosynthetic rate at optimum temperature (A_{opt}), and the thermal breadth (T_{br}).

Species	T_{max} (°C)		T_{opt} (°C)		A_{opt} ($\mu\text{mol CO}_2 \text{ m}^{-2} \text{ s}^{-1}$)		T_{br} (°C)	
<i>A. clivicola</i>	39.67	± 1.65	27.05	$\pm 0.85^*$	9.30	$\pm 0.81^*$	11.28	± 0.90
<i>A. deserticola</i>	46.01	± 2.07	29.63	$\pm 0.62^*$	19.64	$\pm 2.54^*$	14.65	± 1.50

Asterisk denotes significant difference between species at $p < 0.05$.

The thermal maximum value where carbon gain reach zero (T_{max}) was higher ($p = 0.0538$) in *A. deserticola* (46.01 °C) compared to *A. clivicola* (36.67 °C). Interestingly, the thermal breadth (T_{br}), which reflects the potential increase in T_{max} with no changes in T_{opt} was similar in both species (Table 1).

2.4. Leaf Mass Per Area and Water Relation Variables

Statistically significant differences ($p < 0.05$) in leaf mass per area (LMA) between species were found, where *A. clivicola* showed higher LMA values (131.95 g m^{-2}) than *A. deserticola* (105.01 g m^{-2}) (Figure 3A). Specifically, both species showed similar values of leaf area, the differences in LMA lying on the greater leaf mass of *A. clivicola*.

Leaf relative water content (RWC) differed between species after HW ($p < 0.05$), being lower in *A. deserticola* (64.4%) than in *A. clivicola* (70.58%) (Figure 3B). RWC was affected in *A. deserticola* after HW, with a decrease of ca. 7%, whereas no change was observed in *A. clivicola*.

Both species showed similar values of leaf water potential at midday (Ψ_{md}) before HW (Figure 3C). However, after HW leaf Ψ_{md} values were lower in *A. deserticola* (−2.49 MPa). Specifically, *A. deserticola* showed a significant decrease of leaf Ψ_{md} of ca. 14% after HW, while leaf Ψ_{md} of *A. clivicola* was not affected by HW.

3. Discussion

In this study, we examined photosynthetic and water relation traits of two *Atriplex* species exposed to a three-day simulated heat wave (HW). In general, photochemistry, carbon metabolism and hydraulics are the processes mostly affected by heat stress during the vegetative phase of plants [12]. Overall, both *Atriplex* species were resistant to high temperatures, an expected feature for C4 plants, which have evolved in warmer and dry environments [17,23]. Nevertheless, the HW had distinctive effects on the photosynthetic and water relation traits of *A. clivicola* and *A. deserticola*, suggesting species-specific mechanisms underlying its remarkable improvement in iWUE. Specifically, the response to the HW of *A. clivicola* was to enhance water saving, whereas the response of *A. deserticola* was to enhance its photosynthetic performance.

Heat stress, alone or combined with other abiotic stress, such as drought, can severely affect the integrity of thylakoid membranes and the function of PSII [38–40]. Our results showed that after HW, there was a reduction in the maximum quantum efficiency of PSII (F_v/F_m) in both *Atriplex* species, although with average values no lower than 0.74 (Figure 1A). These results reflect that the maximum quantum yield capacity of photosystem

II was not severely affected by the heat stress in either species. By contrast, the actual quantum yield (Φ_{PSII}) was more sensitive to heat stress, particularly in *A. deserticola*. It has been reported that negative effects on photochemistry and light-energy partition, particularly on F_v/F_m and Φ_{PSII} , are apparently temporal, and recovery may occur rapidly in sensitive plants, such as soybean, whereas even positive effects have been observed in heat-tolerant plants [38,41]. Notably, we observed for both *Atriplex* species an increase in F_0 after the heat wave, but contrary to what is expected; it was accompanied by an increase in F_m [42]. Indeed, a higher increase of F_m in *A. deserticola* would explain the reduction of its quantum yield of energy dissipation (F_0/F_m) and sustain its actual quantum yield after HW. Together, these results suggest that, after three days of heat stress, the integrity of thylakoid membranes would be barely impaired, and the photosynthetic machinery remains functional.

Here, the values obtained for NPQ components q_E , q_P and q_L reveal different mechanisms in the *Atriplex* species to deal with light energy after HW (Figure 1D–F). Specifically, the higher values of q_E in *A. clivicola* suggest that HW would affect the capability of the photochemical apparatus to use light energy in photochemistry and must activate the components that rapidly relax high-energy state quenching in order to drain the excess of light energy and avoid potential photoinhibition and photo-oxidative stress [43–45]. On the other hand, HW did not alter the photosystem functioning of *A. deserticola*, which maintained q_P and q_L values without significant variations compared to those observed before HW and were comparatively higher than those of *A. clivicola* after HW. Since these two components reflect the partition of light energy into photochemistry (q_P) and the fraction of open PSII centers with oxidized QA (q_L), we can infer that the thylakoid membranes and proteins of *A. deserticola* remain stable and functional after three days of high temperature. The latter would support the observation that ETR did not change in *A. deserticola* with HW and was higher than *A. clivicola* after heat stress. Similar results have been reported in high-temperature resistant cultivars of wheat and quinoa [38,46], which suggests that the ability to increase chlorophyll content under heat stress is pivotal to diminishing heat damage of thylakoid membranes and enhances the efficiency of electron transport at high temperatures. Although here, we did not measure chlorophyll content; there was no visual evidence of chlorosis during and after HW. In sum, a hypothesis derived from our results is that, under heat stress, *A. deserticola* would either increase chlorophyll content or show a rapid turnover of chlorophyll, whereas *A. clivicola* would use photoprotective mechanisms mainly associated with the xanthophyll cycle to deal with excess light energy.

It is considered that extreme supra-optimal temperatures usually restrict photosynthesis by affecting chloroplasts membrane fluidity and protein stability, enzyme properties, and decreasing CO_2 solubility and stomatal aperture, with a further decrease of CO_2 flux [22,41,47]. Again, the results of temperature–response curves and gas exchange support the notion that *A. clivicola* and *A. deserticola* are high-temperature resistant plants. Despite differences between both *Atriplex* species, they have high photosynthetic optimum temperatures compared to other woody plant species [48]. The maximum photosynthetic capacity (A_{max}) of *A. clivicola* was not affected by HW despite a significant reduction in stomatal conductance (g_s), whereas an increase of A_{max} was observed in *A. deserticola* without evident changes in g_s . Both species reduced the apparent transpiration rate (E) while significantly enhancing their intrinsic water use efficiency (iWUE). Similar results have been reported in drought-tolerant crop varieties [39]. Additionally, Eustis et al. [38] found that heat stress alone increased carbon assimilation in several quinoa genotypes but, contrary to our findings, at the expense of higher stomatal conductance and plant water demand. Heat-induced limiting carbon assimilation is mainly due to the impairment of electron transport and Rubisco activase capacity [15]. Hence, in the case of *A. deserticola*, the increase in A_{max} can be partly explained by the ability to maintain the efficiency of the photochemical process and ETR after HW, as mentioned above. The fact that both species had high LMA values can be related to our observed A_{max} values since leaf size and thickness are key traits in the response of leaf photosynthesis to heat and thermal

sensitivity [13,32,49]. Indeed, in a Mediterranean sclerophyllous ecosystem, plants with thicker leaves were less affected by a two-days heat wave ($>45\text{ }^{\circ}\text{C}$) than plants with larger and thinner leaves [50].

The evaporative demand of water increases with temperature; therefore, leaf hydraulic responses are important to cope with the increase of leaf-to-air vapor pressure deficit [51]. Coordination between leaf hydraulics and leaf gas exchange is key for the balance of carbon gain and water loss [52,53]. Here, the relative water content (% RWC) and leaf water potential (Ψ_{md}) of *A. clivicola* were insensitive to heat waves, whereas *A. deserticola* displayed a significant decrease in both parameters (Figure 3B,C). Given that the former showed a reduction of g_s after HW, this helps the plant decrease leaf evaporative water loss and would partly explain the RWC values observed after the heat stress, which in turn would contribute to keeping leaf water potential. On the other hand, the fact that g_s of *A. deserticola* was insensitive to HW, a higher evaporative water loss would be a plausible explanation for the reduction in RWC and Ψ_{md} . However, given that A_{max} increased while E decreased compared to the values before HW, leaf water loss would be within a tolerable margin that would not jeopardize carbon assimilation and water use efficiency.

Environmental gradients shape the expression of ecophysiological traits [54,55]. Our results can be associated with the local environmental conditions within the species' altitudinal distribution. *A. clivicola* is a coastal lowland species, whereas *A. deserticola* inhabits high-altitude ecosystems of the Andean range. This distribution imposes marked differences regarding microclimatic conditions, such as thermal amplitude, solar radiation and air humidity. The zone in which *A. clivicola* is distributed has a strong ocean influence, low thermal oscillation, and there is an important contribution of fog as a source of water for plants [56–58]. Therefore, avoidance of water loss under a heat wave is to be expected. On the other hand, *A. deserticola* must face high thermal amplitude within a single day, along with high irradiation [59]. Additionally, in high-mountain habitats, low partial pressure of gases and windy days may affect CO_2 availability [60]. Thus, it is reasonable to expect that *A. deserticola* would show better photosynthetic performance under heat stress. Therefore, the contrasting ecophysiological strategies exhibited by *A. clivicola* and *A. deserticola* are consistent with the adaptation of each species to their local environmental conditions at different altitudes. Notably, despite the above-mentioned differences, both species coordinate their photosynthetic and water relation traits to enhance water use efficiency under heat stress.

4. Materials and Methods

4.1. Plant Material and Growth Conditions

One-year-old plants of *A. clivicola* and *A. deserticola* were obtained from the nursery garden of the Chilean Forestry Institute (INFOR-Sede Diaguaita, La Serena, Chile). Plants were propagated vegetatively and, once rooted, placed on individual plastic bags of $20\text{ cm} \times 20\text{ cm}$ filled with organic potting mix. The plants were watered thrice a week during spring and summer and twice a week during autumn–winter. Once well established, during spring, a total of 60 plants ($n = 30$ per species) were transferred to a greenhouse at Universidad de La Serena, Campus Andres Bello ($29^{\circ}54'53.04''\text{ S } 71^{\circ}14'31.22''\text{ W}$). Plants were watered at field capacity thrice a week, based on the values obtained by a Time Domain Reflectometer soil moisture meter TDR350 (FieldScout Spectrum Technologies, Inc., Aurora, IL, USA). The greenhouse roof was covered by a white polyethylene sheet providing ca. $800\text{--}1200\text{ }\mu\text{mol photons m}^{-2}\text{ s}^{-1}$ at solar midday. All ecophysiological traits described below were evaluated before and after the simulated heat wave.

4.2. Heat Wave Simulation

We selected twelve healthy plants per species in order to submit them to a three-day simulated heat wave. Plants were transferred to a growth chamber of 12 m^2 with controlled temperature and light conditions. The temperature control consists of a cooling system of a 2 hp condensing unit coupled with heat convection plates controlled by the software

Sitrad Pro (www.sitrad.com.br, accessed on 24 November 2022, Full Gauge Controls, Canoas, RS, Brazil). The light was provided by 1000 W RGB LED panels. Plants were preconditioned to the chamber conditions under 25 °C and 16/8 h day/night during a week. Plants were placed on metal racks, each with three LED panels 50 cm above the top of the plants, to ensure a homogeneous light distribution. The PAR (photosynthetically active radiation) provided by the led panels was of ca. 400 $\mu\text{mol photons m}^{-2} \text{s}^{-1}$. Watering was at field capacity, as described above. After the preconditioning period, the chamber temperature was set to 28 °C night, 33 °C from 6 to 11 am, and 38 °C during the rest of the day (Supplemental Dataset S1), according to the 16/8 h day/night photoperiod indicated above. To define the heat wave conditions, we analyzed 20 years of data on the absolute maximum temperature during spring–summer (CEAZA meteorological stations network; www.ceazamet.cl, accessed on 24 November 2022). The 3 d duration of the simulated heat wave followed the IPCC definition [61].

4.3. Chlorophyll Fluorescence and Gas Exchange

Chlorophyll fluorescence measurements were conducted with an FMS2 pulse-modulated fluorometer (Hansatech Instruments Ltd., Norfolk, UK) to determine the dark-adapted parameters and NPQ components. The actinic light used was 400 $\mu\text{mol quanta m}^{-2} \text{s}^{-1}$. Forty-eight leaves (two leaves per individual, a total of 24 individuals) were dark-adapted overnight prior to measurements. The maximum and actual quantum yield of PSII (Fv/Fm and ΦPSII), the quantum yield of energy dissipation (Fo/Fm), non-photochemical quenching (NPQ) and the electron transport rate (ETR) were calculated as described in Maxwell and Johnson [62,63]. NPQ components (qE, qI and qL) were calculated from Fm' dark relaxation kinetics after high light exposure for 1 h, as described by Bravo et al. [64] and Bascuñán-Godoy et al. [65] with slight modifications.

Leaf gas exchange measurements were conducted using a gas exchange system (LI-6400, Li-Cor Inc., Lincoln, NE, USA) with a leaf chamber of 2 cm² with a LED light source (LI-6400-40). We conducted light response curves on three individuals per species to determine the light saturation point for both *Atriplex* species. CO₂ concentration was set at 400 ppm, and nine consecutive light steps of 10 min each to ensure CO₂ assimilation was stable were set as follows: 0, 50, 100, 300, 500, 900, 1200, 1500 and 2000 $\mu\text{mol photons m}^{-2} \text{s}^{-1}$ [66]. Leaves were carefully placed in the sensor head, ensuring contact with the leaf thermocouple. A picture of each leaf inside the chamber's gasket was taken to determine the leaf area and subsequently use it to calculate gas exchange parameters. Light-saturated CO₂ assimilation (A_{max}), stomatal conductance (g_s), and apparent transpiration rate (E) were measured in twelve individuals per species from 9:00 to 13:00. Gas exchange parameters were recorded 10 min after clamping the leaf. Leaf chamber conditions were set at 400 ppm of CO₂, 1200 $\mu\text{mol photons m}^{-2} \text{s}^{-1}$ (90:10% red: blue light), 60–65% relative humidity and 25 °C block temperature. For each gas exchange measurement, the intrinsic water use efficiency (iWUE) was calculated as the ratio of photosynthesis (A_{max}) over stomatal conductance (g_s).

We conducted leaf temperature response curves to determine the optimum photosynthetic temperature (T_{opt}), the temperature compensation point (T_{max}), and the photosynthetic thermal breadth (T_{br}). We used five individuals of each *Atriplex* species for measurements of net photosynthesis temperature (A-T) response curves (Supplemental Figure S1). A-T curves were performed between 09:00 to 14:00 h on healthy, fully expanded leaves using an open gas exchange system (Li-6400XT, Li-Cor Inc., Lincoln, NE, USA), equipped with a water bath and a temperature expansion kit to reach both lowest (<15 °C) and highest temperatures (>36 °C), set at 1500 $\mu\text{mol photons m}^{-2} \text{s}^{-1}$ (10% blue), an ambient CO₂ concentration of 400 mmol CO₂ mol⁻¹, and with 12 different block temperatures (12 °C, 15 °C, 18 °C, 21 °C, 24 °C, 27 °C, 30 °C, 33 °C, 36 °C, 40 °C, 45 °C and, 50 °C). The relative humidity (RH) of the sample was regulated to 50 ± 0.5% during measurements except at block temperatures >36 °C, where it was allowed to drop to avoid condensation damage within the IRGA [67]. Once parameters were at steady-state for at least 6 min for each block

temperature, we recorded leaf temperature (T_{leaf}) and photosynthetic rate (A_{net}). Then, to determine the temperature at the carbon compensation point (T_{max}), the temperature at optimum photosynthesis (T_{opt}), the photosynthetic rate at optimum temperature (A_{opt}), and the breadth of temperature optimum (T_{span}), we fit the data using a standard quadratic equation [67] as $A_{\text{net}} = aT_{\text{leaf}}^2 + bT_{\text{leaf}} + c$, where A_{net} is net photosynthesis ($\mu\text{mol m}^{-2} \text{s}^{-1}$) at T_{leaf} ($^{\circ}\text{C}$), and a , b and c are coefficients that describe the A-T response. Curves were fitted using linear models with quadratic components ($Y_i = \beta_0 + \beta_1 X_i + \beta_2 X_i^2 + \epsilon_i$), using T_{leaf} as the independent variable (X_i) and A_{net} as the dependent variable using the “lm” function in the ‘stats’ package in R version 4.0.0 [68].

4.4. Leaf Mass Per Area, Relative Water Content and Leaf Water Potential

Leaf samples employed for gas exchange and chlorophyll fluorescence measurements (24 samples per species) were used to determine the dry leaf mass per unit area (LMA) and relative water content (RWC %). LMA was calculated as the ratio between the dry leaf weight and leaf area obtained through the ImageJ software version 1.54e (ImageJ; nih.gov, accessed on 23 November 2022), according to Perez-Harguindeguy et al. ([69]). RWC of each leaf was determined as in Ostria-Gallardo et al. [70]: % RWC = $((Fw - Dw)/(Tw - Dw)) \times 100$; where Fw = fresh weight, Dw = dry weight, and Tw = turgid weight. The turgid weight was obtained by dipping the leaf into a 2 mL Eppendorf tube full of distilled water and storing it at 4 $^{\circ}\text{C}$ for 24 h prior to weighing.

For leaf water potential (Ψ_{md} , MPa) at midday (11:00–14:00), a healthy apical branch of each individual ($n = 24$) was detached using a fresh razor blade, immediately wrapping the cut end with a wet paper and storing it in a sealed dark plastic bag with a moist paper towel. We measured Ψ_{md} (MPa) using a Scholander-type pressure chamber (PMS Instrument Company, Corvallis, OR, USA) 10–45 min after sample collection.

4.5. Data Analysis

Data were checked for normality assumptions and variance homoscedasticity with the InfoStat software [71]. Accordingly, the parametric one-way ANOVA or non-parametric Kruskal–Wallis analyses were used to compare means within species and between species separately. When significant differences were found, we used post hoc tests with Tukey or pairwise comparisons ($p \leq 0.05$), depending on the parametric or non-parametric nature of the data.

5. Conclusions

Based on their photosynthetic and water relation traits, both *Atriplex* species enhanced their water-use efficiencies after a three-days heat wave treatment (HW). This enhancement was governed by different mechanisms depending on the species. *A. clivicola* achieved it by enhancing water saving by closing stomata and maintaining the leaf RWC (%) and Ψ_{md} at similar values to those registered before HW. By contrast, *A. deserticola* enhanced its photosynthetic performance at the expense of water loss at the foliar level. Specifically, after HW, *A. deserticola* showed an increase of A_{max} without evident changes in stomatal conductance and with higher values of chlorophyll fluorescence parameters associated with photochemistry and electron transport.

It is expected that heat waves and other extreme climatic events associated with climate change will become more frequent and intense. Here we provide evidence of different ecophysiological strategies to cope with heat waves in desert shrubs, which are keystone species for plant diversity and ecosystem function, and hence it is essential to understand the mechanisms by which they deal with climate change.

Supplementary Materials: The following supporting information can be downloaded at: <https://www.mdpi.com/article/10.3390/plants12132464/s1>, Figure S1: Leaf temperature response curves; Supplemental Dataset S1: Growth chamber settings.

Author Contributions: Conceptualization, E.O.-G.; methodology, E.O.-G., E.Z.-C. and D.E.C.; formal analysis, E.O.-G. and D.E.C.; investigation, E.O.-G., T.C.d.L.P., E.G. and L.B.-G.; resources, E.O.-G. and D.E.C.; data curation, E.O.-G., E.Z.-C. and D.E.C.; writing—original draft preparation, E.O.-G.; writing—review and editing, E.Z.-C., D.E.C., T.C.d.L.P., E.G. and L.B.-G.; visualization, E.O.-G.; supervision, E.O.-G.; project administration, E.O.-G.; funding acquisition, E.O.-G. and D.E.C. All authors have read and agreed to the published version of the manuscript.

Funding: This research was funded by Agencia Nacional de Investigación y Desarrollo (ANID), Fondecyt Iniciación N°11201086. D.E.C was funded by Fondecyt Postdoctoral N°3230154, Project ANID FB210006, and Project FONDAP-ANID 152A0001. The APC was funded by Project Fondecyt Iniciación N°11201086.

Data Availability Statement: Data are available on request from the authors.

Acknowledgments: E.O.-G. Thanks, José Hernández from the Chilean Forestry Institute, for kindly providing the plant material used in this work. E.O.-G. thanks, Jaume Flexas, León Bravo and Jeroni Galmes, for their valuable comments and suggestions on the data and methodological advice. D.E.C. acknowledge the support of Instituto de Ecología y Biodiversidad (IEB) and Centro de Ciencia del Clima y la Resiliencia (CR2).

Conflicts of Interest: The authors declare no conflict of interest.

References

1. Noy-Meir, I. Desert ecosystems: Environment and producers. *Annu. Rev. Ecol. Syst.* **1973**, *4*, 25–51. [[CrossRef](#)]
2. Ward, D. *The Biology of Deserts*; Oxford University Press: Oxford, UK, 2016.
3. Maestre, F.T.; Valladares, F.; Reynolds, J.F. Is the change of plant–plant interactions with abiotic stress predictable? A meta-analysis of field results in arid environments. *J. Ecol.* **2005**, *93*, 748–757. [[CrossRef](#)]
4. Horton, J.L.; Hart, S.C. Hydraulic lift: A potentially important ecosystem process. *Trends Ecol. Evol.* **1998**, *13*, 232–235. [[CrossRef](#)] [[PubMed](#)]
5. Parmesan, C. Ecological and evolutionary responses to recent climate change. *Annu. Rev. Ecol. Syst.* **2006**, *37*, 637–669. [[CrossRef](#)]
6. Mora, C.; Caldwell, I.R.; Caldwell, J.M.; Fisher, M.R.; Genco, B.M.; Running, S.W. Suitable days for plant growth disappear under projected climate change: Potential human and biotic vulnerability. *PLoS Biol.* **2015**, *13*, e1002167. [[CrossRef](#)]
7. Becklin, K.M.; Anderson, J.T.; Gerhart, L.M.; Wadgymar, S.M.; Wessinger, C.A.; Ward, J.K. Examining plant physiological responses to climate change through an evolutionary lens. *Plant Physiol.* **2016**, *172*, 635–649. [[CrossRef](#)] [[PubMed](#)]
8. Archer, S.R.; Andersen, E.M.; Predick, K.I.; Schwinning, S.; Steidl, R.J.; Woods, S.R. Woody plant encroachment: Causes consequences. In *Rangeland Systems*; Briske, D.D., Ed.; Springer: Berlin/Heidelberg, Germany, 2017; pp. 25–84.
9. Ramachandran, A.; Praveen, D.; Jaganathan, R.; RajaLakshmi, D.; Palanivelu, K. Spatiotemporal analysis of projected impacts of climate change on the major C3 and C4 crop yield under representative concentration pathway 4.5: Insight from the coasts of Tamil Nadu, South India. *PLoS ONE* **2017**, *12*, e0180706.
10. Sage, R.F. Global change biology: A primer. *Glob. Chang. Biol.* **2019**, *26*, 3–30. [[CrossRef](#)] [[PubMed](#)]
11. Coumou, D.; Rahmstorf, S. A decade of weather extremes. *Nat. Clim. Chang.* **2012**, *2*, 491–496. [[CrossRef](#)]
12. Balfagón, D.; Zandalinas, S.I.; Mittler, R.; Gómez-Cadenas, A. High temperatures modify plant responses to abiotic stress conditions. *Physiol. Plant.* **2020**, *170*, 335–344. [[CrossRef](#)]
13. Breshears, D.D.; Fontaine, J.B.; Ruthrof, K.X.; Field, J.P.; Feng, X.; Burger, J.R.; Law, D.; Kala, J.; Hardy, G.E. Underappreciated plant vulnerabilities to heat waves. *New Phytol.* **2020**, *231*, 32–39. [[CrossRef](#)] [[PubMed](#)]
14. He, Y.; Fang, J.; Xu, W.; Shi, P. Substantial increase of compound droughts and heatwaves in wheat growing seasons worldwide. *Int. J. Climatol.* **2022**, *42*, 5038–5054. [[CrossRef](#)]
15. Sage, R.F.; Kubien, D.S. The temperature response of C3 and C4 photosynthesis. *Plant Cell Environ.* **2007**, *30*, 1086–1107. [[CrossRef](#)]
16. Segovia, R. Temperature predicts maximum tree-species richness and water availability and frost shape the residual variation. *Ecology* **2023**, *104*, e4000. [[CrossRef](#)] [[PubMed](#)]
17. Hoover, D.L.; Knapp, A.L.; Smith, M.D. Contrasting sensitivities of two dominant C4 grasses to heat waves and drought. *Plant Ecol.* **2014**, *215*, 721–731. [[CrossRef](#)]
18. Thompson, V.; Kennedy-Asser, A.T.; Vosper, E.; Eunice Lo, Y.T.; Huntingford, C.; Andrews, O.; Collins, M.; Hegerl, G.C.; Mitchell, D. The 2021 western North America heat wave among the most extreme events ever recorded globally. *Sci. Adv.* **2022**, *8*, eabm6860. [[CrossRef](#)]
19. Aparecido, L.M.T.; Woo, S.; Suazo, C.; Hultine, K.R.; Blonder, B. High water use in desert plants exposed to extreme heat. *Ecol. Lett.* **2020**, *23*, 1189–1200. [[CrossRef](#)]
20. Marchin, R.M.; Backes, D.; Ossola, A.; Leishman, M.R.; Tjoelker, M.G.; Ellsworth, D.S. Extreme heat increases stomatal conductance and drought-induced mortality risk in vulnerable plant species. *Glob. Chang. Biol.* **2021**, *28*, 1133–1146. [[CrossRef](#)]
21. Sage, R.F.; Monson, R.K. (Eds.) *C4 Plant Biology*; Academic Press: San Diego, CA, USA, 1999; p. 597.

22. Dusenage, M.E.; Duarte, A.G.; Way, D.A. Plant carbon metabolism and climate change: Elevated CO₂ and temperature impacts on photosynthesis, photorespiration and respiration. *New Phytol.* **2018**, *221*, 32–49. [[CrossRef](#)]
23. Sage, R.F.; Christin, P.-A.; Edwards, E.J. The C₄ plant lineages of planet Earth. *J. Exp. Bot.* **2011**, *62*, 3155–3169. [[CrossRef](#)]
24. Čalasan, A.Ž.; Hammen, S.; Sukhorukov, A.P.; McDonald, J.T.; Brignone, N.F.; Böhnert, T.; Kadereit, G. From continental Asia into the world: Global historical biogeography of the saltbush genus *Atriplex* (Chenopodiaceae, Amaranthaceae). *Perspect. Plant Ecol. Evol. Syst.* **2022**, *54*, 125660. [[CrossRef](#)]
25. Kiani-Pouya, A.; Roessner, U.; Jayasinghe, N.S.; Lutz, A.; Rupasinghe, T.; Bazihizina, N.; Bohm, J.; Alharbi, S.; Hedrich, R.; Shabala, S. Epidermal bladder cells confer salinity stress tolerance in the halophyte quinoa and *Atriplex* species. *Plant Cell Environ.* **2017**, *40*, 1900–1915. [[CrossRef](#)] [[PubMed](#)]
26. Feng, S.; Wang, B.; Li, C.; Guo, H.; Bao, A.-K. Transcriptomic analysis provides insight into the ROS scavenging system and regulatory mechanisms in *Atriplex canescens* response to salinity. *Int. J. Mol. Sci.* **2023**, *24*, 242. [[CrossRef](#)]
27. Slatyer, R.O. Comparative photosynthesis, growth and transpiration of two species of *Atriplex*. *Planta* **1970**, *93*, 175–189. [[CrossRef](#)] [[PubMed](#)]
28. Mooney, H.A.; Ehleringer, J.; Björkman, O. The energy balance of leaves of the evergreen desert shrub *Atriplex hymenelytra*. *Oecologia* **1977**, *29*, 301–310. [[CrossRef](#)] [[PubMed](#)]
29. Martinez, J.P.; Ledent, J.F.; Bajji, M.; Kinet, J.M.; Lutts, S. Effect of water stress on growth, Na⁺ and K⁺ accumulation and water use efficiency in relation to osmotic adjustment in two populations of *Atriplex halimus* L. *Plant Growth Regul.* **2003**, *41*, 63–73. [[CrossRef](#)]
30. Belkheiri, O.; Mulas, M. Effect of water stress on growth, water use efficiency and gas exchange as related to osmotic adjustment of two halophytes *Atriplex* spp. *Funct. Plant Biol.* **2013**, *40*, 466–474. [[CrossRef](#)]
31. Taiz, L.; Zeiger, E. *Plant Physiology*, 5th ed.; Benjamin/Cummings Series; Benjamin Cummings Publishing Company: San Francisco, CA, USA, 2010; p. 559.
32. Lambers, H.; Chapin, F.S., III; Pons, T.L. *Plant Physiological Ecology*; Springer: Berlin/Heidelberg, Germany, 2008; p. 604.
33. Qiu, N.; Lu, C. Enhanced tolerance of photosynthesis against high temperature damage in salt-adapted halophyte *Atriplex centralasiatica* plants. *Plant Cell Environ.* **2003**, *26*, 1137–1145. [[CrossRef](#)]
34. Piticar, A. Changes in heat waves in Chile. *Glob. Planet. Chang.* **2018**, *169*, 234–246. [[CrossRef](#)]
35. Burger, F.; Brock, B.; Montecinos, A. Seasonal and elevational contrast in temperature trends in central Chile between 1979 and 2015. *Glob. Planet. Chang.* **2018**, *162*, 136–147. [[CrossRef](#)]
36. Rosas, M.R. The genus *Atriplex* (Chenopodiaceae) in Chile. *Gayana Bot.* **1989**, *46*, 3–82.
37. Rodríguez, R.; Marticorena, C.; Alarcón, D.; Baeza, C.; Cavieres, L.; Finot, V.L.; Fuentes, N.; Kiessling, A.; Mihoc, M.; Pauchard, A.; et al. Catálogo de las plantas vasculares de Chile. *Gayana Bot.* **2018**, *75*, 1–430. [[CrossRef](#)]
38. Eustis, A.; Murphy, K.M.; Barrios-Masias, F. Leaf gas Exchange performance of ten quinoa genotypes under a simulated heat wave. *Plants* **2020**, *9*, 81. [[CrossRef](#)] [[PubMed](#)]
39. Killi, D.; Raschi, A.; Bussotti, F. Lipid peroxidation and chlorophyll fluorescence of photosystem II performance during drought and heat stress is associated with the antioxidant capacities of C₃ sunflower and C₄ maize varieties. *Int. J. Mol. Sci.* **2020**, *21*, 4846. [[CrossRef](#)] [[PubMed](#)]
40. Zhu, L.; Wen, W.; Thorpe, M.R.; Hocart, C.H.; Song, X. Combining heat stress with pre-existing drought exacerbated the effects on chlorophyll fluorescence rise kinetics in four contrasting plant species. *Int. J. Mol. Sci.* **2021**, *22*, 10682. [[CrossRef](#)]
41. Siebers, M.H.; Yendrek, C.R.; Drag, D.; Locke, A.M.; Rios-Acosta, L.; Leakey, A.D.B.; Ainsworth, E.A.; Bernacchi, C.J.; Ort, D.R. Heat waves imposed during early pod development in soybean (*Glycine max*) cause significant yield loss despite a rapid recovery from oxidative stress. *Glob. Chang. Biol.* **2015**, *21*, 3114–3125. [[CrossRef](#)] [[PubMed](#)]
42. Martinazzo, E.G.; Ramm, A.; Bacarin, M.A. The chlorophyll a fluorescence as an indicator of the temperature stress in the leaves of *Prunus persica*. *Braz. J. Plant Physiol.* **2012**, *24*, 237–246. [[CrossRef](#)]
43. Demmig-Adams, B. Carotenoids and photoprotection in plants: A role for the xanthophyll zeaxanthin. *Biochim. Biophys. Acta BBA Bioenerg.* **1990**, *1020*, 1–24. [[CrossRef](#)]
44. Murchie, E.H.; Ruban, A.V. Dynamic non-photochemical quenching in plants: From molecular mechanisms to productivity. *Plant J.* **2020**, *101*, 885–896. [[CrossRef](#)]
45. Colpo, A.; Baldisserotto, C.; Pancaldi, S.; Sabhia, A.; Ferroni, L. Photosystem II inhibition and photoprotection in a lycophyte, *Selaginella martensii*. *Physiol. Plant.* **2022**, *174*, e13604. [[CrossRef](#)]
46. Sharma, D.K.; Andersen, S.B.; Ottosen, C.O.; Rosenqvist, E. Wheat cultivars selected for high Fv/Fm under heat stress maintain high photosynthesis, total chlorophyll, stomatal conductance, transpiration and dry matter. *Physiol. Plant.* **2015**, *153*, 284–298. [[CrossRef](#)]
47. Lobo, A.K.M.; Catarino, I.C.A.; Silva, E.A.; Centeno, D.C.; Domingues, D.S. Physiological and molecular responses of woody plants exposed to future atmosphere CO₂ levels under abiotic stresses. *Plants* **2022**, *11*, 1880. [[CrossRef](#)] [[PubMed](#)]
48. Lin, Y.-S.; Medlyn, B.E.; Ellsworth, D.S. Temperature responses of leaf net photosynthesis: The role of component processes. *Tree Physiol.* **2012**, *32*, 219–231. [[CrossRef](#)]
49. Münchinger, I.K.; Hajek, P.; Akdogan, B.; Caicoya, A.T.; Kunert, N. Leaf thermal tolerance and sensitivity of temperature tree species are correlated with leaf physiological and functional drought resistance traits. *J. For. Res.* **2023**, *34*, 63–76. [[CrossRef](#)]

50. Groom, P.K.; Lamont, B.B.; Leighton, S.; Leighton, P.; Burrows, C. Heat damage in sclerophylls is influenced by their leaf properties and plant environment. *Écoscience* **2004**, *11*, 94–101. [[CrossRef](#)]
51. Yang, Y.; Zhang, Q.; Huang, G.; Peng, S.; Li, Y. Temperature responses of photosynthesis and leaf hydraulic conductance in rice and wheat. *Plant Cell Environ.* **2020**, *43*, 1437–1451. [[CrossRef](#)]
52. Xiong, D.; Flexas, J. Safety-efficiency tradeoffs? Correlations of photosynthesis, leaf hydraulics, and dehydration tolerance across species. *Oecologia* **2022**, *200*, 51–64. [[CrossRef](#)]
53. de Sousa-Leite, T.; Oliveira de Freitas, R.M.; da Silva-Dias, N.; Dallabona-Dombroski, J.L.; Nogueira, N.W. The interplay between leaf water potential and osmotic adjustment on photosynthetic and growth parameters of tropical dry forest trees. *J. For. Res.* **2023**, *34*, 177–186. [[CrossRef](#)]
54. Carvajal, D.E.; Loayza, A.P.; Rios, R.S.; Gianoli, E.; Squeo, F.A. Population variation in drought-resistance strategies in a desert shrub along an aridity gradient: Interplay between phenotypic plasticity and ecotypic differentiation. *Perspect. Plant Ecol. Evol. Syst.* **2017**, *29*, 12–19. [[CrossRef](#)]
55. Wang, J.; Wen, X. Limiting resource and leaf functional traits jointly determine distribution patterns of leaf intrinsic water use efficiency along aridity gradients. *Front. Plant Sci.* **2023**, *13*, 909603. [[CrossRef](#)]
56. Larrain, H.; Velásquez, F.; Cereceda, P.; Espejo, R.; Pinto, R.; Osses, P.; Schemenauer, R.S. Fog measurements at the site “Falda Verde” north of Chañaral compared with other fog stations of Chile. *Atmos. Res.* **2002**, *64*, 273–284. [[CrossRef](#)]
57. Cereceda, P.; Larrain, H.; Osses, P.; Fariás, M.; Egaña, I. The climate of the coast and fog zone in the Tarapacá Region, Atacama Desert, Chile. *Atmos. Res.* **2008**, *87*, 301–311. [[CrossRef](#)]
58. Stotz, G.C.; Salgado-Luarte, C.; Vigil, A.T.; De La Cruz, H.J.; Pastén-Marambio, V.; Gianoli, E. Habitat-islands in the coastal Atacama Desert: Loss of functional redundancy, but not of functional diversity, with decreased precipitation. *Ann. Bot.* **2021**, *127*, 669–680. [[CrossRef](#)] [[PubMed](#)]
59. Montecinos, S.; Gutiérrez, J.R.; López-Cortés, F.; López, D. Climatic characteristics of the semi-arid Coquimbo Region in Chile. *J. Arid Environ.* **2016**, *126*, 7–11. [[CrossRef](#)]
60. Liu, W.; Zheng, L.; Qi, D. Variation in leaf traits at different altitudes reflects the adaptive strategy of plants to environmental changes. *Ecol. Evol.* **2020**, *10*, 8166–8175. [[CrossRef](#)]
61. Seneviratne, S.I.; Zhang, X.; Adnan, M.; Badi, W.; Dereczynski, C.; Di Luca, A.; Ghosh, S.; Iskandar, I.; Kossin, J.; Lewis, S.; et al. *Weather Climate Extreme Events in a Changing Climate In Climate Change 2021: The Physical Science Basis Contribution of Working Group I to the Sixth Assessment Report of the Intergovernmental Panel on Climate Change*; Masson-Delmotte, V., Zhai, P., Pirani, A., Connors, S.L., Péan, C., Berger, S., Caud, N., Chen, Y., Goldfarb, L., Gomis, M.I., et al., Eds.; Cambridge University Press: Cambridge, UK, New York, NY, USA; 2021; pp. 1513–1766. [[CrossRef](#)]
62. Maxwell, K.; Johnson, G.N. Chlorophyll fluorescence—A practical guide. *J. Exp. Bot.* **2000**, *51*, 659–668. [[CrossRef](#)]
63. Kramer, D.M.; Johnson, G.; Kiirats, O.; Edwards, G.E. New fluorescence parameters for the determination of Q(A) redox state and excitation energy fluxes. *Photosynth. Res.* **2004**, *79*, 209–218. [[CrossRef](#)]
64. Bravo, L.A.; Saavedra-Mella, F.; Vera, F.; Guerra, A.; Cavieres, L.A.; Ivanov, A.G.; Huner, N.P.A.; Corcuera, L.J. Effect of cold acclimation on the photosynthetic performance of two ecotypes of *Colobanthus quitensis* (Kunth) Bartl. *J. Exp. Bot.* **2007**, *58*, 3581–3590. [[CrossRef](#)]
65. Bascuñán-Godoy, L.; Sanhueza, C.; Cuba, M.; Zúñiga, G.E.; Corcuera, L.J.; Bravo, L.A. Cold-acclimation limits low temperature induced photoinhibition by promoting a higher photochemical quantum yield and a more effective PSII restoration in darkness in the Antarctic rather than the Andean ecotype of *Colobanthus quitensis* Kint Bartl (Caryophyllaceae). *BMC Plant Biol.* **2012**, *12*, 114.
66. Gago, J.; Nadal, M.; Clemente-Moreno, M.J.; Figueroa, C.M.; Medeiros, D.B.; Cubo-Ribas, N.; Cavieres, L.A.; Gulías, J.; Fernie, A.R.; Flexas, J.; et al. Nutrient availability regulates *Deschampsia antarctica* photosynthetic and stress tolerance performance in Antarctica. *J. Exp. Bot.* **2023**, *74*, ead043. [[CrossRef](#)]
67. Docherty, E.M.; Gloor, E.; Sponchiado, D.; Gilpin, M.; Pinto, C.A.D.; Junior, H.M.; Coughlin, I.; Ferreira, L.; Junior, J.A.S.; da Costa, A.C.L.; et al. Long-term drought effects on the thermal sensitivity of Amazon Forest trees. *Plant Cell Environ.* **2023**, *46*, 185–198. [[CrossRef](#)] [[PubMed](#)]
68. R Core Team. *R: A Language and Environment for Statistical Computing*; R Foundation for Statistical Computing: Vienna, Austria, 2023; Available online: <https://www.R-project.org/> (accessed on 9 May 2023).
69. Pérez-Harguindeguy, N.; Díaz, S.; Garnier, E.; Lavorel, S.; Poorter, H.; Jaureguiberry, P.; Bret-Harte, M.S.; Cornwell, W.K.; Craine, J.M.; Gurvich, D.E.; et al. Corrigendum to: New handbook for standardized measurement of plant functional traits worldwide. *Aust. J. Bot.* **2016**, *64*, 715–716. [[CrossRef](#)]
70. Ostria-Gallardo, E.; Larama, G.; Berríos, G.; Fallard, A.; Gutiérrez-Moraga, A.; Ensminger, I.; Bravo, L.A. A comparative gene co-expression analysis using self-organizing maps on two congener filmy ferns identifies specific desiccation tolerance mechanisms associated to their microhabitat preference. *BMC Plant Biol.* **2020**, *20*, 56. [[CrossRef](#)] [[PubMed](#)]
71. Di Renzo, J.; Casanoves, F.; Balzarini, M.; Gozález, L.; Tablada, M.; Robledo, C. *InfoStat Versión 2014*; InfoStat Group, FCA, Universidad Nacional de Córdoba: Córdoba, Argentina, 2014.

Disclaimer/Publisher’s Note: The statements, opinions and data contained in all publications are solely those of the individual author(s) and contributor(s) and not of MDPI and/or the editor(s). MDPI and/or the editor(s) disclaim responsibility for any injury to people or property resulting from any ideas, methods, instructions or products referred to in the content.